VAN DER WAALS HETEROSTRUCTURES

Multifunctional devices from asymmetry

A heterostructure made from various two-dimensional materials can be used to build a device that functions as a diode, transistor, photodetector and non-volatile memory.

Yanqing Wu

Two-dimensional semiconductors can confine charge carriers within an atomic-layer thickness and thus serve as the thinnest possible channel materials. Such capabilities can provide efficient electrostatic control in scaled-down devices, where undesired leakage current between source and drain electrodes can cause power dissipation when in standby. These materials can also be stacked to create a diverse range of layered heterostructures — also known as van der Waals heterostructures. These heterostructures can combine different two-dimensional materials, and their associated properties, in a way that would be prohibited by natural crystal growth due to lattice mismatch, allowing new material systems with new functionalities to be created.

Despite the significant potential of these structures, there is currently a considerable gap between the capabilities of the intrinsic materials and the actual performance of the resulting heterostructure devices. In the development of future electronic devices it will also be important that the heterostructures offer performance that is either higher than state-of-the-art silicon complementary metal–oxide–semiconductor (CMOS) devices, or with multi-purpose application with a higher level of integration than silicon CMOS devices. Previous work on two-dimensional heterostructure devices has demonstrated promising memory and logic functions[1–3], but the performance and capabilities of these devices remains limited. Writing in *Nature Electronics*, Jun He and colleagues now show that an asymmetric van der Waals heterostructure device can function as a diode, transistor, photodetector and non-volatile memory[4].

The researchers — who are based at the CAS Center for Excellence in Nanoscience in Beijing and the University of Chinese Academy of Science in Beijing — built heterostructure devices on SiO_2/Si substrates using graphene, hexagonal boron nitride, molybdenum disulfide (MoS_2) and molybdenum ditelluride ($MoTe_2$). The graphene acts as the gate electrode at the bottom of the device, hexagonal boron nitride as an insulating dielectric, MoS_2 as a lateral channel, and a $MoTe_2$/MoS_2 vertical heterojunction acts as a channel at the top (Fig. 1a). In this asymmetric three-terminal heterostructure, the ambipolar nature of $MoTe_2$ plays an essential role in the electrical transport of the device, allowing it to switch from n-type to p-type when the gate bias changes from positive to negative. The MoS_2 channel, on the other hand, operates as a unipolar n-channel device, which switches off at negative bias and switches on at positive gate bias, just like in a classical n-type transistor. As a result, the $MoTe_2$/MoS_2 heterostructure can operate both as an n–n and p–n junction, depending on the gate voltage, and rectifying behaviour can be achieved at a specific voltage window.

It is also possible to control the carrier injection by applying a bias at the drain terminal, due to the asymmetric nature of the device. In this case, most of the voltage bias across the channel can be applied either at the vertical heterojunction or at the lateral MoS_2 channel, creating a large electric field. More specifically, this large electric field across the heterojunction under

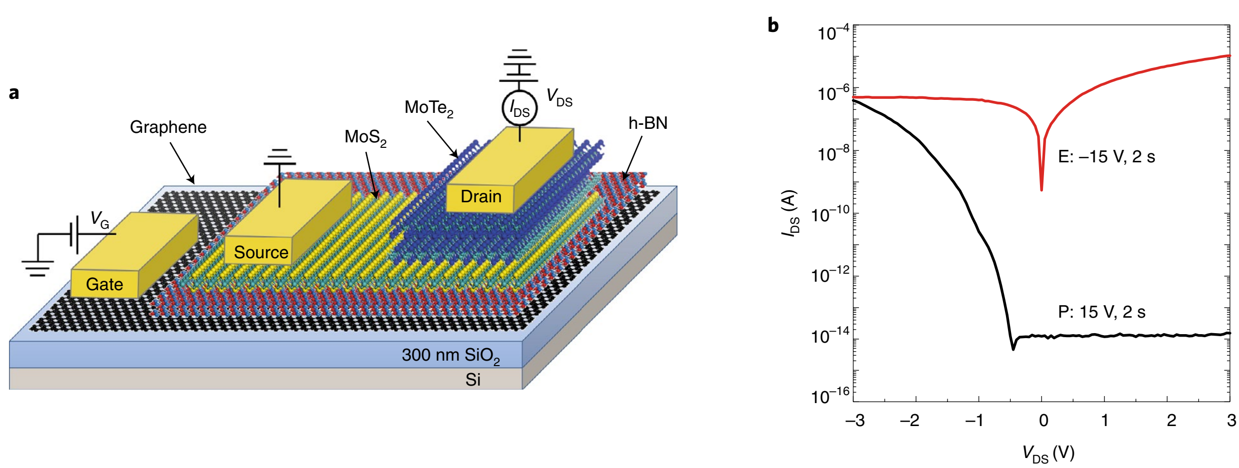

Fig. 1 | **Multifunctional asymmetric van der Waals heterostructure devices. a**, Schematic of the van der Waals heterostructure device, which is made from various two-dimensional materials — graphene, hexagonal boron nitride (h-BN), molybdenum disulfide (MoS_2) and molybdenum ditelluride ($MoTe_2$) — assembled on a SiO_2/Si substrate. I_{DS}, drain to source current; V_{DS}, drain to source voltage; V_G, gate voltage. **b**, Electrical characterization of the non-volatile programmable rectifier. The black and red curves represent the program (P) and erase (E) states of the device, respectively. Credit: reproduced from ref. [4], Macmillan Publishers Ltd.

reverse bias will make the energy barrier sufficiently narrow and allow a large current to flow via electron tunnelling. In contrast, under positive bias the transport mode changes and the heterojunction becomes a vertical channel with minimal current flow from tunnelling. With this approach, He and colleagues are able to achieve a record high current on/off ratio of 6×10^8 and a rectifying ratio of more than 10^8. This is due, in particular, to the well-defined bandgap alignment and efficient gate control from using boron nitride as an insulating layer. Building such p–n junctions with ultrathin materials enables non-classical electronic transport, and is a key advantage over conventional materials like silicon, where achieving an ultra-shallow vertical junction with the required doping profiles is enormously challenging. Similar transport behaviour could also be obtained by constructing p–n heterojunctions using other ambipolar two-dimensional semiconductors such as black phosphorus.

Based on the asymmetric transport behaviour, the researchers also explored the gate-tunable photoresponse of the device. High external quantum efficiency with minimal dark current was achieved when the p–n heterostructure at the drain side was in forward bias. The rectifying transport mode of the heterostructures also created a strong photovoltaic effect, which suggests the devices have significant potential in future optoelectronics applications. While graphene was used in these applications only as a gate electrode, the researchers also showed that it could act as a charge-storing floating gate for non-volatile memory applications when a back-gate voltage is applied using the silicon substrate. With this configuration, the rectifying transport behaviour was used to create a multi-bit programmable rectifier that can preserve and control multiple memory states (Fig. 1b). The combination of a very low current at the p–n heterojunction under forward drain bias and a negatively charged floating gate means that the leakage charge flow is minimal. As a result, the device exhibits a remarkably low program current and a record-high program/erase current ratio of 10^9. The high program/erase ratio provides a large current window in which to create multiple states between high and low resistance states. It was thus possible to achieve four well-separated memory states by tuning the graphene Fermi level using different back-gate voltage pulses and durations.

The approach of He and colleagues offers both multifunctionality and high performance, thanks to the versatile nature of two-dimensional van der Waals heterostructures. As with any new material system, delivering industrial applications will mean addressing significant challenges in terms of larger-scale production of such devices while maintaining uniformity and reliability. For electronics, it is also important to consider the potential for integration with existing silicon platforms and the related process and thermal budget compatibility. The two-dimensional materials community has recently achieved rapid progress in the synthesis of lateral and vertical heterostructures[5–7]. Furthermore, high-throughput computational approaches have been adopted to identify potential new two-dimensional materials[8], and robotic systems have been developed to search for and assemble complex van der Waals heterostructures[9]. These advances suggest that the multifunctional heterostructures of He and colleagues could have a promising future in the development of practical electronic devices. ❐

Yanqing Wu
Wuhan National High Magnetic Field Center and School of Electrical and Electronic Engineering, Huazhong University of Science and Technology, Wuhan, China.
e-mail: yqwu@mail.hust.edu.cn

Published online: 13 June 2018
https://doi.org/10.1038/s41928-018-0093-1

References

1. Li, D. et al. *Nat. Nanotech.* **12**, 901–906 (2017).
2. Huang, M. et al. *Nat. Nanotech.* **12**, 1148–1154 (2017).
3. Liu, C. et al. *Nat. Nanotech.* **13**, 404–410 (2018).
4. Cheng, R. et al. *Nat. Electron*. https://doi.org/10.1038/s41928-018-0086-0 (2018).
5. Sahoo, K. P., Memaran, S., Xin, Y., Balicas, L. & Gutiérrez, H. R. *Nature* **553**, 63–67 (2018).
6. Zhang, Z. et al. *Science* **357**, 788–792 (2017).
7. Zhou, J. et al. *Nature* **556**, 355–359 (2018).
8. Mounet, N. et al. *Nat. Nanotech.* **13**, 246–252 (2018).
9. Masubuchi, S. et al. *Nat. Commun.* **9**, 1413 (2018).